Yuzuncu Yil University
Journal of the Institute of Natural & Applied Sciences
https://dergipark.org.tr/en/pub/yyufbed

Research Article

Synthesis, Characterization, Antimicrobial Activities and Molecular Docking Studies of Nanoparticles from *Polygonum cognatum, Mentha pulegium* and *Tragopogon reticulatus*

Saniye ASLAN[1], Yunus BAŞAR[2], Aybek YİĞİT[*1]

[1]Igdir University, Tuzluca Vocational School, Pharmacy Services Department, 76000, Igdir, Türkiye
[2]Igdir University, Research Laboratory Practice and Research Center, 76000, Igdir, Türkiye
* Corresponding author e-mail: aybek.yigit@igdir.edu.tr

Abstract: Nanotechnology and its applications are increasing day by day in the food industry, medicine, pharmacy, cosmetics and industrial sectors as technology develops. However, research into their impact on human health and nature continues. In this study, Ag, Cu and Fe nanoparticles (NPs) were obtained from the plants *Polygonum cognatum*, *Mentha pulegium,* and *Tragopogon reticulatus* by methanol extracts and green synthesis. The characteristic properties of these synthesized particles were tested by FE-SEM, FESEM-EDX, UV-Vis, FT-IR and HPLC. The antimicrobial activities of the extracts and NPs obtained against the microorganisms *Staphylococcus aureus*, *Enterococcus faecalis* and *Pseudomonas aeruginosa* were tested using the disk diffusion method. Also, the inhibitory properties of the molecules and NP complexes identified in HPLC analysis against the enzyme topoisomerase IV were theoretically calculated by molecular docking. In HPLC analysis, chlorogenic acid (*P. cognatum* and *T. reticulatus)* and chrysin (*M. pulegium*) were detected in the highest amounts. In studies on antibacterial activity, all NPs obtained from *P. cognatum, M. pulegium* and *T. reticulatus* showed activity against *S. aureus*. According to the molecular docking result, chlorogenic acid-AgNP and chrysin-CuNP had higher MolDock values. As a result, the NPs and extracts made from these plants have use in medicine, food, and cosmetics.

Keywords: Antibacterial, *Mentha pulegium,* Molecular docking, Nanoparticle, *Polygonum cognatum, Tragopogon reticulatus*

Polygonum cognatum, Mentha pulegium ve *Tragopogon reticulatus*'tan Elde Edilen Nanopartiküllerin Sentezi, Karakterizasyonu, Antimikrobiyal Aktiviteleri ve Moleküler Yerleştirme Çalışmaları

Özet: Nanoteknoloji ve uygulamaları, teknoloji geliştikçe gıda endüstrisi, tıp, eczacılık, kozmetik ve endüstriyel sektörlerde her geçen gün artmaktadır. Ancak, insan sağlığı ve doğa üzerindeki etkilerine yönelik araştırmalar devam etmektedir. Bu çalışmada, *Polygonum cognatum, Mentha pulegium* ve *Tragopogon reticulatus* bitkilerinden metanol ekstraktları ve yeşil sentez yoluyla Ag, Cu ve Fe nanopartikülleri elde edildi. Sentezlenen bu partiküllerin karakteristik özellikleri FE-SEM, FESEM-EDX, UV-Vis, FT-IR ve HPLC ile belirlendi. Elde edilen ekstrakt ve nanopartiküllerin *Staphylococcus aureus, Enterococcus faecalis* ve *Pseudomonas aeruginosa* mikroorganizmalarına karşı antimikrobiyal aktiviteleri disk difüzyon yöntemi kullanılarak test edildi. Ayrıca HPLC analizinde belirlenen moleküllerin ve molekül-partikül komplekslerinin topoizomeraz IV enzimine karşı inhibitör özellikleri moleküler yerleştirme yoluyla teorik olarak hesaplandı. HPLC analizinde, *P. cognatum* ve *T. reticulatus*'ta klorojenik asit, *M. pulegium*'da chrysin en fazla miktarda tespit edildi. Antibakteriyel aktivite üzerine yapılan çalışmalarda, *P. cognatum*, *M. pulegium* ve *T. reticulatus*'tan elde edilen tüm nanopartiküllerin *S. aureus*'a karşı etki gösterdi. Moleküler yerleştirme sonucuna göre, klorojenik asit-AgNP ve crysin-AuNP'nin daha yüksek MolDock değerleri vardı. Sonuç olarak, bu bitkilerden elde edilen ekstraktlar ve NP'ler gıda, farmakoloji ve kozmetik gibi alanlarda kullanılabilir.

Anahtar Kelimeler: Antibakteriyel, *Mentha pulegium,* Moleküler yerleştirme, Nanopartikül, *Polygonum cognatum, Tragopogon reticulatus*

Received: 16.01.2025
Accepted: 17.04.2025

How to cite: Aslan, S., Başar, Y., & Yiğit, A. (2025). Synthesis, characterization, antimicrobial activities and molecular docking studies of nanoparticles from *Polygonum Cognatum, Mentha Pulegium* and *Tragopogon Reticulatus*. *Yuzuncu Yil University Journal of the Institute of Natural and Applied Sciences*, *30*(2), 537-554. https://doi.org/10.53433/yyufbed.1621096

1. Introduction

Nanotechnology is a new field that deals with the structures created by the coming together of molecules and atoms on the nanoscale (Phan & Haes, 2019). Nanomaterials used in nanotechnology can occur in nature or be obtained by various methods in a laboratory environment. In NPs: bottom-up production, which starts from atoms and molecules, and top-down production, which makes it possible to achieve smaller structures by separating large parts (Wolfgang, 2007). In NPs, large-sized materials are broken down into smaller nano-sized materials by various methods (Duncan, 2011). As a result of this decomposition, NPs are synthesized. NPs are synthesized from plants, algae, bacteria, and fungi. The biological synthesis method is a method that has been widely used in recent years due to its low cost, lack of toxic catalysts, and ease of use (Gavande et al., 2016).

Tragopogon reticulatus, species known to the public as 'Manger' and belonging to the daisy family, grows in the Eastern Black Sea, Upper Euphrates, Erzurum-Kars-Ağrı, Hakkari regions of Turkey. Its long, carrot-like black roots and new shoots taste like oysters and are edible. Chewing gum can be made from the milky sap that oozes from the stem. The plant is often used by the public for its anti-inflammatory and diuretic effects. One study found that cribwort leaves are a good source of glutathione, β-carotene, vitamin C, vitamins B2, B3, and B6 and are a powerful antioxidant due to their high phenolic and flavonoid content (Çöteli & Karataş, 2015). *Mentha pulegium*, popularly known as 'Yarpuz' or 'Filiskin', is a perennial, herbaceous, creeping or upright-stemmed plant of the Lamiaceae family, 10 to 50 cm tall, with purple petals, flowers in separate rings, a pungent, mint-like odor and hazelnut-like fruits. Used by the Greeks and Romans in cooking and to sweeten wine, pennyroyal has an antimicrobial effect and has been used throughout history as a purifying medicine to treat sinusitis, cholera, food poisoning, fainting, flatulence, bile, gout, and hepatitis (Hadi et al., 2017; Miraj & Kiani, 2016). *Polygonum cognatum* is a perennial edible herbaceous plant of the sorrel family (Polygonaceae) with a woody stem that creeps along the ground and has small pink flowers. It is not only used as a food, but is also one of the plants that is frequently consumed because its antioxidant effect protects the body from harmful free radicals and has a positive effect on stomach and intestinal health (Çoban et al., 2021; Eruygur et al., 2020).

Bacterial resistance to known antibacterial agents requires the development of new antibacterial compounds with novel mechanisms of action that target new targets and act against resistant bacterial strains (Kato, 2008). Topoisomerase IV is a vital bacterial enzyme that unwinds newly replicated DNA and enables the segregation of daughter chromosomes. In order to discover antibacterial agents, inhibitors that would switch off the effect of bacterial topoisomerase IV are being investigated (Skvarča, 2019).

Molecular modeling methods are computational method used to support experimental studies. They are generally used in fields such as chemistry and pharmacy to predict the results that can be obtained without in vivo and in vitro experiments. The aim here is to determine the stable conformation of the ligand by determining the protein-ligand interactions. In this way, the inhibitory properties of the molecule are also determined (Pinzi & Rastelli, 2019; Erenler et al., 2024; Yildiz et al., 2024).

In our study, particles containing the metals Ag (AgNPs), Fe (FeNPs), and Cu (CuNPs) were synthesized from the extracts of the plants *P. cognatum*, *T. reticulatus,* and *M. pulegium*. *T. reticulatus* particles containing the metals Ag, Fe and Cu were synthesized for the first time. The characteristic properties of the syntheses were determined such as Scanning Electron Microscope (SEM), fourier transform infrared spectroscopy (FTIR), and ultraviolet–visible (UV-Vis). Also, the antibacterial properties of the extract and the NPs were determined using the disk diffusion method. The synthesis of *T. reticulatus*-NPs was investigated for the first time. In addition, the phenol content of the extracts obtained was determined using high-performance liquid chromatography (HPLC) and, the interactions of the molecules identified as the main components in the HPLC analysis and their molecular synthesis structures against the enzyme topoisomerase IV [4URN] isolated from *S.aureus* were calculated theoretically by molecular docking. In this way, it will provide a perspective on the use of plants in areas such as food, cosmetics, and pharmacology.

2. Material and Methods

2.1. Chemicals

Ultrapure water, methanol, ethanol, iron (III) chloride hexahydrate ($FeCl_3.6H_2O$), silver nitrate ($AgNO_3$), and copper (II) nitrate trihydrate (Cu $(NO_3)_2$ $3H_2O$) were provided by companies Sigma-Aldrich and Merck Millipore.

2.2. Plants

The plants of *M. pulegium, T. reticulatus* and *P. cognatum* were acquired in dried form in the province of Ağrı in Turkey. The species identification of the plants was carried out by Prof. Dr. Ahmet Zafer TEL from the Faculty of Agriculture of Iğdır University, Department of Agricultural Biotechnology. The plants were then ground and stored in the refrigerator for analysis.

2.3. Extraction

After being thoroughly cleaned with ultrapure water, the plants were dried for 72 hours at 25 ºC temperature in an oven before being ground to a powder using a grinder. The extraction procedures were then initiated. Twenty grams of each plant were extracted and put into three separate 250 mL Erlenmeyer flasks. Each Erlenmeyer flask was then filled with 100 mL of methanol and heated to approximately 85 ºC for 15 minutes at 1500 rpm. The sample in the Erlenmeyer was covered with aluminum foil to ensure complete protection from the sun. Filtration was performed on the Erlenmeyer flasks following the heating procedure. The filtration process was applied to three different plant species sequentially and the obtained extracts were stored in a refrigerator at +4 ºC for later use (Başar et al., 2024a).

2.4. Synthesis of AgNP

Green synthesis AgNPs were created using a more practical technique that has no negative impacts and no natural additives. A 250 mL erlenmeyer flask was filled with a 100 ml aqueous solution of 10 mM $AgNO_3$ made with pure water. After that, 80 mL of previously made plant extracts were added to the $AgNO_3$ solution, which had been fully covered with aluminum foil and swirled on a magnetic stirrer for 16 hours at 250 rpm and 25 ºC. The centrifugation procedure was then initiated. The solid sample that remained after washing (3000 rpm, 10 minutes) was thoroughly dried in an oven set at 60 ºC for 24 hours in order to be used for characterization. Pure water was added twice throughout the centrifugation process, and either methyl or ethyl alcohol was added once. All three samples were subjected to these procedures (Öztürk et al., 2020).

2.5. Synthesis of FeNP

As per the protocol, a 0.6 M 100 mL $FeCl_3$ solution was made using ultrapure water for the synthesis of FeNP. The liquid was then heated sufficiently to dissolve all of the solid ingredients and agitated for 15 minutes with a magnetic stirrer until it was fully dissolved. After that, the solution was supplemented with 80 milliliters of $FeCl_3$ solution and 20 milliliters of plant extract. After being heated for four hours at 60 °C in an entirely sealed water bath (aluminum foil), the resultant solution was allowed to cool to ambient temperature for two hours while being stirred. The centrifugation stage was initiated for the obtained solution at the conclusion of this time. During the centrifugation process, the solution was washed with water and ethyl alcohol (4000 rpm/5 min). Following centrifugation, it was then allowed to dry in an oven set at a low temperature for characterization. For every plant sample, these procedures were used consistently (Katata-Seru et al., 2018; Rathore & Devra, 2022).

2.6. Synthesis of CuNP

CuNPs were prepared by mixing 5 mL of the plant extract with 50 mL of an aqueous solution of 10 mM copper nitrate in a 100 mL Erlenmeyer flask while stirring continuously at 100-120 °C with a magnetic stirrer. The color of the reaction mixture changed. After being stirred vigorously for 24 hours,

the color of the reaction mixture changed from dark blue to colorless, then to brick red, and finally to dark red. The resulting solution was then centrifuged for 10 minutes at room temperature at 10,000 rpm. After the collected CuNPs were allowed to dry on a watch glass, the resulting black precipitate was crushed for further analysis (Kumar et al., 2015).

2.7. Characterizations

2.7.1. UV-Vis spectroscopy

The absorption spectra of the extract, CuNPs, AgNPs and FeNPs were analysed with the Agilent Cary 60 UV-Vis absorption spectrophotometer (wavelength: 200-800 nm). The obtained extract and NPs absorption peaks were displayed. The optical band gap was calculated according to formula 1.

$$(\alpha h\nu) = A(h\nu - Eg)^n \quad (1)$$

A is a constant, hν is the photon energy, Eg is the optical band gap and α is the absorption coefficient. The indirect transition is represented by the parameter (n = 1/2), while the direct allowed electron transition is represented by the value (n = 2). The difference between $\alpha h\nu^2$ Vs hν is displayed.

2.7.2. FT-IR spectroscopy

The FT-IR device was used to determine which functional groups were significantly bound to the surface of AgNPs, CuNPs, FeNPs and contributed to the production of AgNPs, CuNPs, FeNPs. The Agilent Cary 630 FT-IR instrument was used for the analyses (Başar et al., 2024a).

2.7.3. Scanning Electron Microscopy (SEM) Analysis

Morphological alterations were determined using a FE-SEM instrument. Using a Zeiss Sigma 300 field emission scanning electron microscope (10kV voltage, X1000).

2.8. Phenolic analysis by HPLC

The crude extract's phenolic content was ascertained using an Agilent 1260 infinite series HPLC. An Acegenerix 5c18 (4.6x250mm) 5µm reversed phase column was installed in the instrument. To get the best separation, the chromatographic parameters were adjusted. The wavelength for the DAD signal was 300/200 nm, with a reference of 500/100 nm. The column's temperature was set to 30 ºC. Water (83%, 85%, 80%, 75%, 70%, 60%, 50%, 30%, 83% at 0, 7, 20, 24, 28, 30, 32, 36, and 40 minutes, respectively) and acetonitrile made up the elution gradient. The injection volume was set at 10 µL, and the solvent flow rate was set at 0.8 mL/min. Furthermore, as standards, 19 phenolic compounds were employed. Twenty milligrams of the extracts were weighed on a precision balance and dissolved in methanol to create the sample. Then, 1 mL was extracted and passed through a 0.45-micron filter. It was injected into the device after being diluted 1:1 with water. The dilution factor was entered as the computation's outcome to complete the calculation (Başar et al., 2024b; Başar et al., 2024a).

2.9. Disk diffusion method for antibacterial activity

The antibacterial activity of NPs and extracts was determined using the Kirby-Bauer method, which is cheap, easy to use and most effective in drug identification. *S. aureus*- ATCC 25923, *E. faecalis*-ATCC 29212, and *P. aeruginosa*-ATCC 27853 microorganisms were used in our study. Gentamicin was selected as the positive group and DMSO (dimethyl sulfoxide) as the negative control group. The study was planned in several steps. In the first step, a stock solution with a concentration of 1024 µg/ml was prepared. In the second step, the microorganisms taken from the stock solution were inoculated into tubes with nutrient broth to produce working cultures. After the microorganisms had been activated in the liquid medium, a Mueller-Hinton agar medium was prepared and sterilized in a third step. After sterilization, approximately 20 ml of agar was poured into each sterilized Petri plate.

The plates were then cooled to allow the agar to solidify. In the fourth step, bacterial suspensions of *S. aureus*, *E. faecalis,* and *P. aeruginosa* prepared according to the 0.5 Mc Farland standard were inoculated onto Mueller-Hinton agar (MHA) and the inoculated bacteria incubated at 37 ºC for 24 hours (Acet & Özcan, 2018; Vakilzadeh et al., 2020). Sterilized plant NPs were weighed and sonicated for 10 to 15 minutes to dissolve them in DMSO. The disk diffusion method (Whatman No. 1) was performed using 6-mm disks, which were sterilized before to use. Separately, DMSO, synthetic NPs, and plant extracts were impregnated onto the sterilized disks. After being submerged in the medium, the impregnated disks and the antibiotic-free disk were incubated for twenty-four hours at 37 °C. To ascertain the antibacterial activity, the disks' zone diameters were measured and tabulated following the incubation.

2.10. Molecular docking studies

In the docking studies, the structure of the chlorogenic acid and chrysin molecules was first drawn in ChemDraw and the minimum energy was calculated with ChemDraw-3D and saved in MOL2 format (Yenigun et al., 2024). The enzyme topoisomerase IV [4URN] isolated from *S. aureus*, whose 3D protein structure we used in our tests, was selected from the RSCB (Protein Data Bank). The program MVD (Molegro Virtual Docker) was used to determine the interaction of the molecule with the active site of the enzyme. The Discovery Studio program was used to view 2D and 3D images of protein-ligand interactions. The images were saved in jpeg format (Başar et al., 2024c; Yildiz et al., 2024).

3. Result and Discussion

In our study, methanol extracts and NPs (Ag, Fe, Cu) were obtained from *P. cognatum*, *T. reticulatus* and *M. pulegium* plants. The characteristic properties, phytochemical content and antibacterial activities of the obtained samples were determined. In addition, the inhibitory properties of chlorogenic acid and crysin molecules, which were observed as the main components in HPLC, against the enzyme topoisomerase IV were calculated theoretically.

3.1. UV-Vis spectroscopy

According to UV-Vis analysis, the extract of *P. cognatum* shows weak peaks at 328, 407 and 663 nm, the extract of *M. pulegium* at 341, 411 and 665 nm and the extract of *T. reticulatus* at 329 and 669 nm (Figure 1). From this, *P. cognatum* extract: 4.98 eV, *M. pulegium extract*: 4.74 eV, *T. reticulatus* extract: 4.96 eV were calculated. In addition, the optical energy band gap of *P. cognatum*-CuNPs was estimated to be 3.67 eV, *M. pulegium*-CuNPs: 3.57 eV, *T. reticulatus*-CuNPs: 3.56 eV. As a result, in UV-Vis spectrophotometric studies, it is observed that CuNPs exhibit absorption bands at different wavelengths, which is a result of the interaction between free electrons on the surface and light of certain wavelengths. This absorption band can be considered to indicate the formation of CuNPs in colloidal solution because it was confirmed in literature studies that CuNPs exhibit characteristic absorption peaks in the range of 200-800 nm (Prema, 2011).

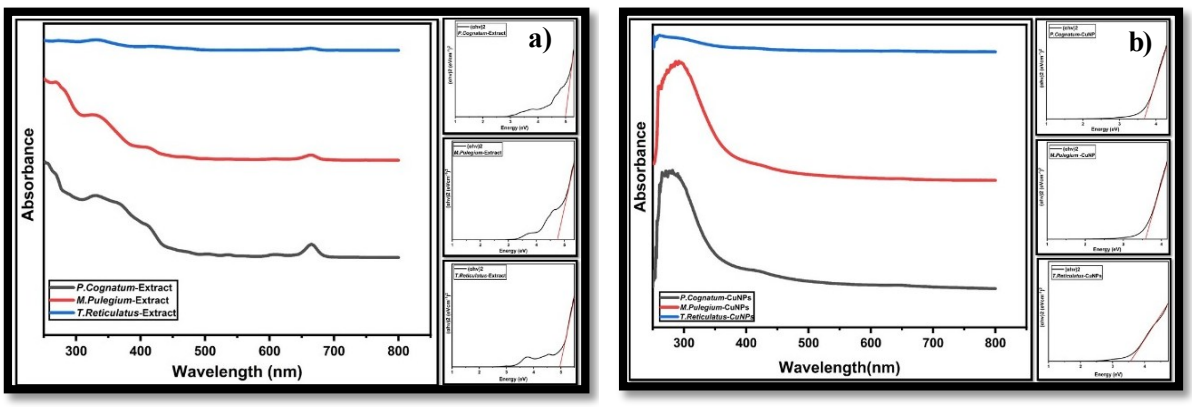

Figure 1. UV-Vis Images of extracts (a) and CuNPs (b).

3.2. FT-IR spectroscopy

According to FT-IR analysis (Figure 2), the broad peak at 3302 cm^{-1} is attributed to stretched hydroxyl groups (OH), which may indicate the presence of phenolic compounds and aromatic alcohols or secondary amide-NH stretching in the leaf extracts (Mahiuddin et al., 2020). The peak at 2345 cm^{-1} is caused by the C-H stretching of the methylene group (Saravanan & Nanda, 2010).

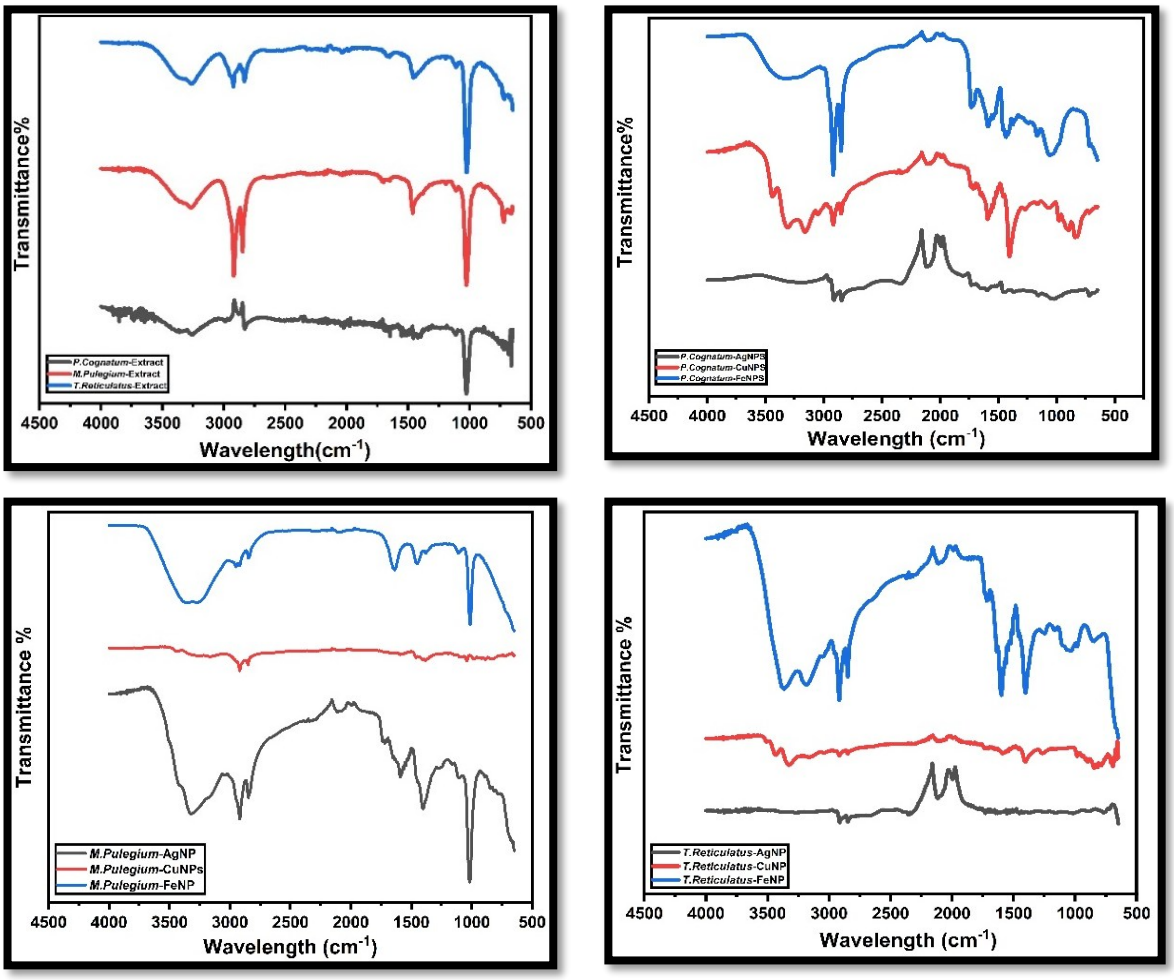

Figure 2. FT-IR images of extracts and NPs.

The vibration band of alkanes (C-H) was linked to the peaks seen at 2917 cm^{-1} and 2847 cm^{-1} (Dinesh et al., 2022). The stretching vibrations of alcohols, carboxylic acids, ethers, esters, and amino acids (-C-O) are assumed to be the cause of the other peak at 1440 cm^{-1} (Chandraker et al., 2019). The stretching vibrations of the proteins (C-OH bond) in the plant extract are linked to the peak at 1014 cm^{-1}. However, the amine (NH_2) and hydroxyl (O–H) bond stretching groups of macromolecular components (cellulose, pectin, polyphenols, etc.) are represented by the broad and flat peak at 3267 cm^{-1} in the AgNPs, FT-IR spectra of NPs derived from *P. cognatum*, and moreover, the stretching vibrations of the methyl, methylene, and methyl groups (C–H) are responsible for the band seen at 2923 cm^{-1} and 2861 cm^{-1} (Kumar et al., 2014). The vibrational bands displayed at 2100, 2899 and 2849 cm^{-1} can be associated with (C-H) groups (Kebede et al., 2024). The biological reduction of Ag^+ ions to Ag^0 NPs may be caused by the primary functional groups in many chemical classes, such as polyphenols, triterpenoids, flavonoids, polysaccharides, etc., according to the results of FT-IR spectra. CuNP spectra show that the following hydroxyl groups may be identified: (-OH) at 3302 and 3153 cm^{-1}, (C-H) at 2923 cm^{-1} and 2861 cm^{-1}, (C=O) at 1559 cm^{-1}, and (-C-O) at 1404 cm^{-1} (Espinoza-Gómez et al., 2020). The hydroxyl groups (-OH) were linked to the peak at 3376 cm^{-1} in the FeNPs spectra, while the C-H groups were linked to the vibration bands at 2911 and 2837 cm^{-1}, the (-C-O) groups to the vibration band at

1429 cm^{-1}, and the (C-O) groups to the vibration band at 1038 cm^{-1} (Jara et al., 2024). Additionally, the vibration band at 3331 cm^{-1} in the AgNPs spectra was attributed to hydroxyl groups (-OH), the vibration bands at 2917 and 2847 cm^{-1} to (C-H) groups, and the vibration band at 1400 cm^{-1} to (-C-O) groups, according to FT-IR analysis of the *M. pulegium*-NPs.

In addition, the band at 1405 cm^{-1} was attributed to the (N-H) stretching vibration, which occurs in the amide bonds of proteins. It can be said that these functional groups play an important role in the stability and coating of AgNPs as reported in many studies (Niraimathi et al., 2013; Prakash et al., 2013). The band at 1043 cm^{-1} was attributed to the stretching vibrations of the proteins (N-H) and (C-N) (amines) (Jyoti et al., 2016). According to the CuNPs spectra, the strong, intense band at 3267 cm^{-1} is attributed to the (–OH) groups in alcohols (Rajesh et al., 2018). The peaks at 2928 and 2835 cm^{-1} were assigned to the (C-H) groups (Amaliyah et al., 2020). According to the FeNPs spectra, the vibration band at 3319 cm^{-1} was associated with the hydroxyl groups (OH) of phenols, the vibration band at 1639 cm^{-1} with the ketone groups (C=O) and the vibration band at 1429 cm^{-1} with the (C=C) groups (Johnson & Uwa, 2019). In addition, the vibration band obtained at 1008 cm^{-1} was associated with the (C–O) groups in polysaccharides, which are frequently found in plants (Mahiuddin et al., 2020). FT-IR analysis of the NPs obtained from *T. reticulatus* revealed that 2888 and 2864, 2100 cm^{-1} in the spectra are assigned to the AgNPs (C-H) groups (Jyoti et al., 2016). In the CuNPs spectra, the strong intense band at 3401 cm^{-1} is attributed to (–OH) groups in alcohols. The peaks at 2059 and 1381 cm^{-1} are associated with (C-H) groups (Amaliyah et al., 2020). According to the FeNPs spectra, the vibration bands at 3378 and 3191 cm^{-1} were associated with hydroxyl groups of phenols (OH) or amines (NH_2), the vibration band at 1598 cm^{-1} with ketones (C=O) groups, the vibration band at 1381 cm^{-1} with (C=C) groups (Mahiuddin et al., 2020). In addition, the vibration band obtained at 1060 cm^{-1} was associated with the (C–O) groups in polysaccharides commonly found in plants (Mahiuddin et al., 2020).

3.3. SEM Results

According to the FE-SEM images of *P. cognatum*, the CuNPs have a spherical and smooth appearance. The EDX of the synthesized CuNPs showed strong copper signals along with Cu and C peaks, which may originate from biomolecules bound to the surface of the CuNPs. In addition, Cu and C contents of 45.63 and 17.25% were detected in the FESEM EDX analyses, respectively (Figure 3). The surface morphology and structure of the NPs were investigated. It was found that the synthesized FeNPs were irregularly shaped, had a rough surface and were not in direct contact, indicating the stabilization of the synthesized NPs. Moreover, some smaller particles with spherical irregular shapes in different sizes are observed in the synthesized FeNPs (Kuang et al., 2013). The FESEM-EDX analysis determined Cu and C contents of 30.46 and 41.26% respectively. The FE-SEM images show that the synthesized CuNPs tend to form spherical and random clusters. In addition, the Cu and C ratios in the FESEM-EDX analysis were determined to be 63.29 and 7.16%, respectively (Amaliyah et al., 2020). *M. pulegium;* The FE-SEM images show that the synthesized CuNPs tend to form spherical and random clusters. In addition, the Cu and C ratios in the FESEM-EDX analysis were determined to be 63.29 and 7.16%, respectively. According to the FE-SEM images, the FeNPs were spherical in shape. In addition, Fe and C ratios of 29.17 and 46.42%, respectively, were determined from the FESEM-EDX spectra (Ardakani et al., 2021). *T. reticulatus*; FE-SEM images of CuNPs taken under the indicated ideal parameters show the production of spherical nanomaterials (Wang et al., 2024). In addition, C:18.40% and Cu:55.22% were detected in the FESEM-EDX spectra (Purniawan et al., 2022). According to the FESEM images of FeNPs, irregular spherical images can be recognized (Xia et al., 2018). In addition, C: 21.69% and Fe: 38.36% were detected in the FESEM-EDX spectra (Nkosinathi et al., 2020).

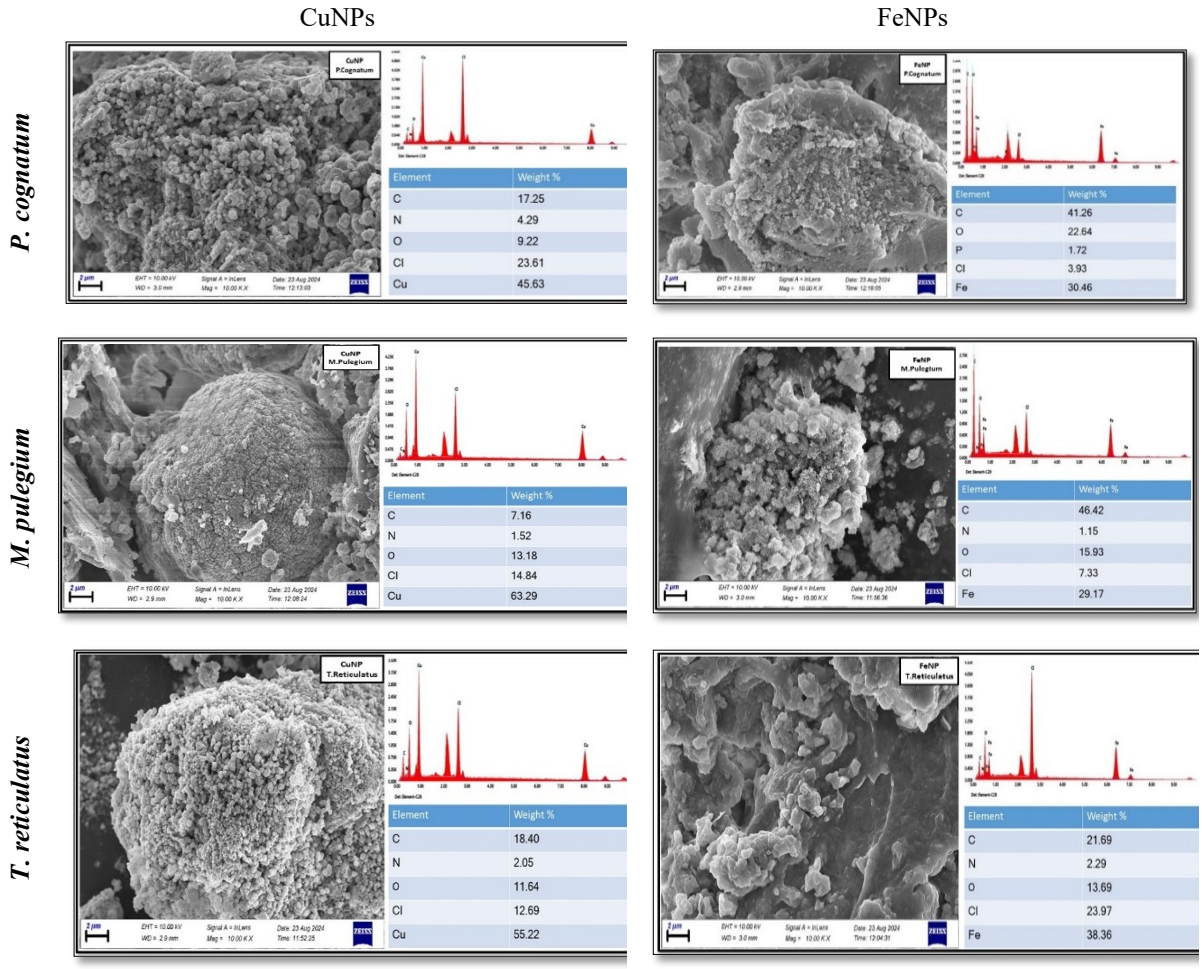

Figure 3. FE-SEM images of NPs of *P. cognatum and M. pulegium.*

3.4. HPLC results of extracts

The phenolic content of the methanol extracts of the plants of *M. pulegium, T. reticulatus* and *P. cognatum* was analyzed by HPLC (Figure 4). According to the analytical results (ng/uL), in *M. pulegium*; chrysin (217.09), o-coumaric acid (42.36), rosmarinic acid (28.19), t-ferulic acid (27.52), naringin (17.98), in *T. reticulatus*; chlorogenic acid (60.55), chrysin (16.56), t-ferulic acid (12.47), 4-hydroxybenzoic acid (10.62), in *P. cognatum*; chlorogenic acid (181.52), catechin hydrate (115.23), rutin (73.38), quercetin (56.70), caffeic acid (33.98) and naringin (16.30) were detected in the highest amounts (Table 1).

Table 1. HPLC analysis results (ng/uL) of the extracts of *P. cognatum, M. pulegium* and *T. reticulatus*

No	Compounds	R.T (min.)	*M. pulegium*	*T. reticulatus*	*P. cognatum*
1	Chlorogenic acid	6.15	6.16	60.55	181.52
2	Catechine hydrate	6.56	-	-	115.23
3	Caffeic acid	9.19	2.73	6.44	33.98
4	4-Hydroxy benzoic acid	13.43	2.96	10.62	-
5	Vanillin	16.76	2.08		8.67
6	p-Coumaric acid	17.30	-	1.13	-
7	Rutin	19.08	5.97	-	73.38
8	*t*-Ferulic acid	20.31	27.52	12.47	-
9	Hydroxy sinamic acid	23.45	3.14	-	2.97
10	Naringin	27.51	17.98	5.59	16.30
11	o-Coumaric acid	28.37	42.36	1.53	4.76
12	Rosmarinic acid	30.05	28.19	1.30	1.30
13	Salicylic acid	31.33	1.36		7.17

Table 1. HPLC analysis results (ng/uL) of the extracts of *P. cognatum, M. pulegium* and *T. reticulatus* (continued)

14	Resveratrol	32.41	-		2.53
15	Quercetin	34.72	3.66	1.08	56.70
16	t-Cinamic acid	35.50	6.28	5.13	-
17	Naringenin	36.31	-	-	8.44
18	Chrysin	39.25	217.09	16.56	-
19	Flavones	40.77	-	-	-

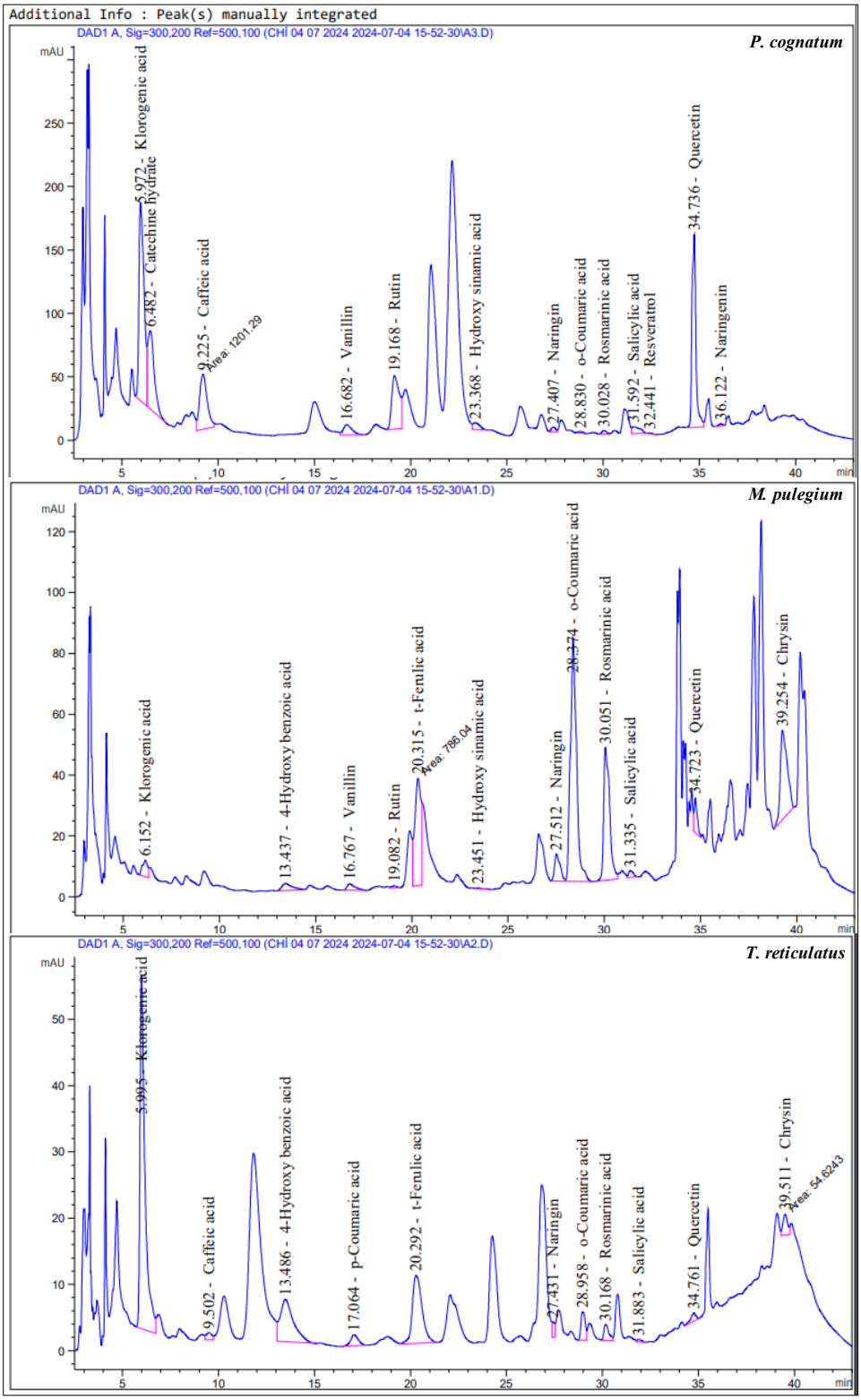

Figure 4. HPLC chromatogram of the extracts of *P. cognatum*, *M. pulegium and T. reticulatus*.

3.5. Antimicrobial activity analysis

Antimicrobial compounds are naturally or synthetically/semi-synthetically derived substances that stop, slow down or even kill the growth of microorganisms such as bacteria, molds, fungi and yeasts. It is now known that thousands of chemical substances in the world have an inhibitory effect on microorganisms. Most of them are natural substances such as plant and animal extracts, tin, mercury and lead (Serpi et al., 2012). The antimicrobial activity of FeNPs, CuNPs, AgNPs and extracts were determined by the disk diffusion method (Figure 5). When investigating the antibacterial activities of methanol extracts and NPs of the *P. cognatum*, *M. pulegium* and *T. reticulatus*, no activity was detected for the extract, while activity was detected for the particles. The CuNP, FeNP and AgNP samples obtained from *P. aeruginos*, *T. reticulatus* and *M. pulegium* showed low activity compared to standard gentamicin. However, *M. pulegium* AgNP (10 mm) also showed good activity against *S. aureus*, *T. reticulatus* FeNP (10 mm) against *E. faecalis* and *M. pulegium* AgNP (9.5 mm) samples showed good activity against *P. aeruginos*. Therefore, it can be said that the *M. pulegium* particles are more effective in terms of antibacterial activity (Table 2) (Manikandan & Sathiyabama, 2015; Okafor et al., 2013). In literature research, similar results were tried against different bacterial groups in antibacterial activity studies and similar results were obtained (Arokiyaraj et al., 2017; Eze et al., 2023).

In conclusion, it can be said that nanoparticles exhibit antimicrobial activity. The reason for this situation has not been clearly determined. However, when extensive studies have been carried out to explain their mode of action, three well-defined mechanisms can be proposed: (i) cell wall and membrane damage, (ii) intracellular penetration and damage, and (iii) oxidative stress (Roy et al., 2019).

Table 2. Zone measurements of antimicrobial activity results obtained using the disk diffusion method

	Organizma	***S. aureus***	***E. faecalis***	***P. aeruginos***
P. cognatum	Extract	_	_	_
	CuNP	7 mm	_	_
	AgNP	7 mm	_	7 mm
	FeNP	7 mm	_	7 mm
T. reticulatus	Extract	_	_	_
	CuNP	6.5 mm	_	_
	AgNP	8 mm	9 mm	_
	FeNP	8 mm	10 mm	_
M. pulegium	Extract	_	_	_
	CuNP	6.5 mm	_	7 mm
	AgNP	10 mm	7.5 mm	9.5 mm
	FeNP	7 mm	_	7.5 mm
Standards	Gentamicin	15 mm	14 mm	15 mm
	DMSO	_	_	_

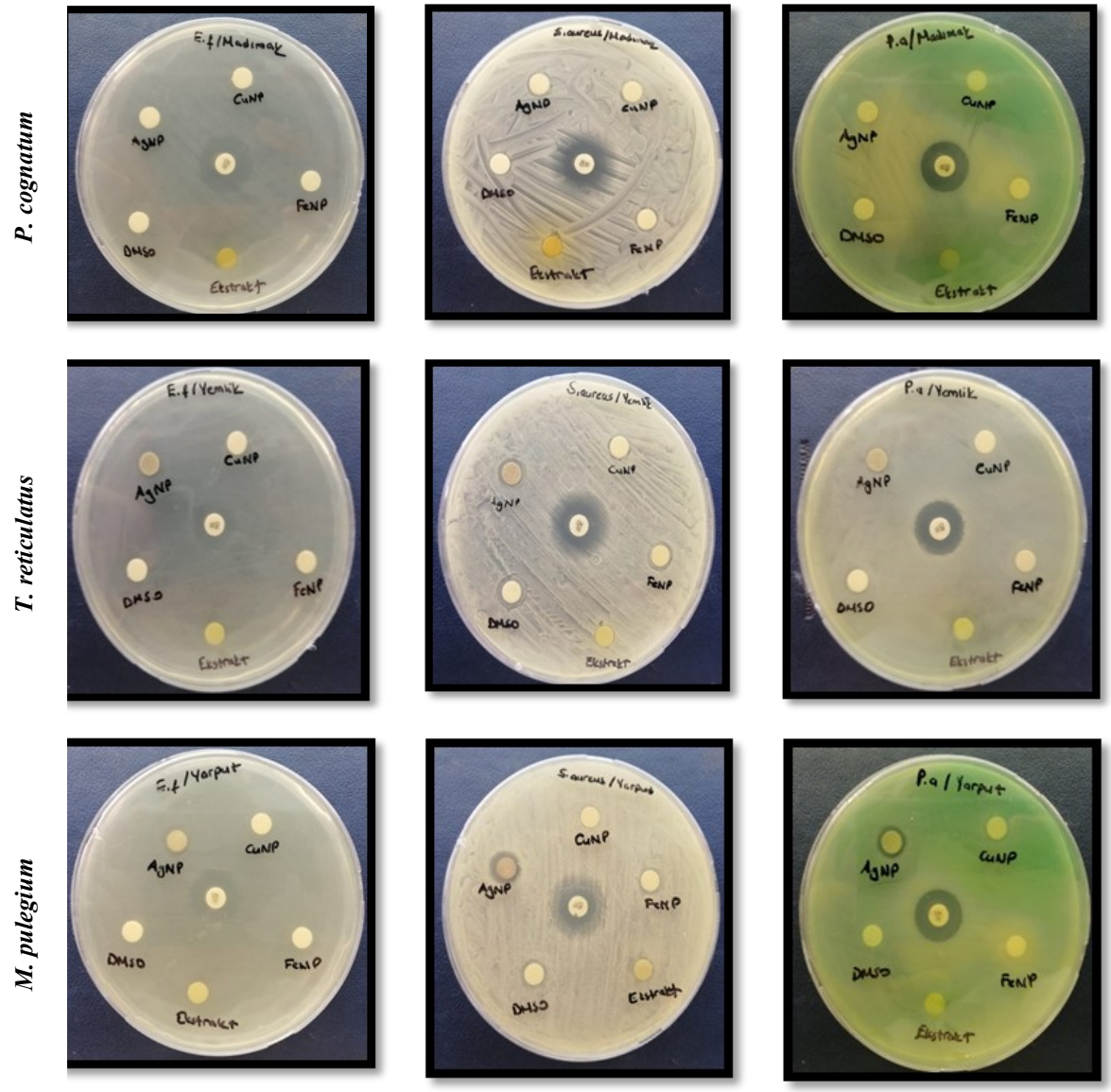

Figure 5. Zone images of NPs, extracts and standards synthesized from *P. cognatum, M. pulegium* and *T. reticulatus* plants against *S. aureus, E. faecalis,* and *P. aeruginosa*.

3.6. Molecular docking studies

Molecular docking simulations are now widely used to study the binding of different types of NPs with proteins and nucleic acids. This not only helps to understand the biological mechanisms of action, but also to predict possible toxicities (Abdelsattar et al., 2021). HPLC analysis of the plants of *P. cognatum, M. pulegium* and *T. reticulatus* was performed. According to the results of the HPLC analysis, the major constituent of *M. pulegium* was chrysin, while the major constituent of *P. cognatum* and *T. reticulatus* was determined to be chlorogenic acid. To estimate the relationship between the antibacterial activities of these major constituents and the topoisomerase IV [4URN] enzymes isolated from *S. aureus*, their interactions were calculated theoretically.

The interactions of chlorogenic acid with the active site of topoisomerase IV identified seven conventional hydrogen bonds (amino acids; GLY80, ASN49, ASP76, THR34 and ILE78), one carbon-hydrogen bond (ASP76) and one pi-alkyl (ALA181) interaction. The MolDock score for the interactions of chlorogenic acid with the enzyme topoisomerase IV was calculated to be-120.658. The chlorogenic acid-AgNP complex was observed to contain seven conventional hydrogen bonds (ARG138, GLY57, LYS36, ARG37), four carbon-hydrogen bonds (HIS41, GLY57, GLY59, ASN60), two pi-cations

(ARG37), one pi-anion (ASP139), two pi-sigma (ARG79, THR166) and two pi-alkyl (ARG79, ARG138) interactions with the active site of the enzyme topoisomerase IV.

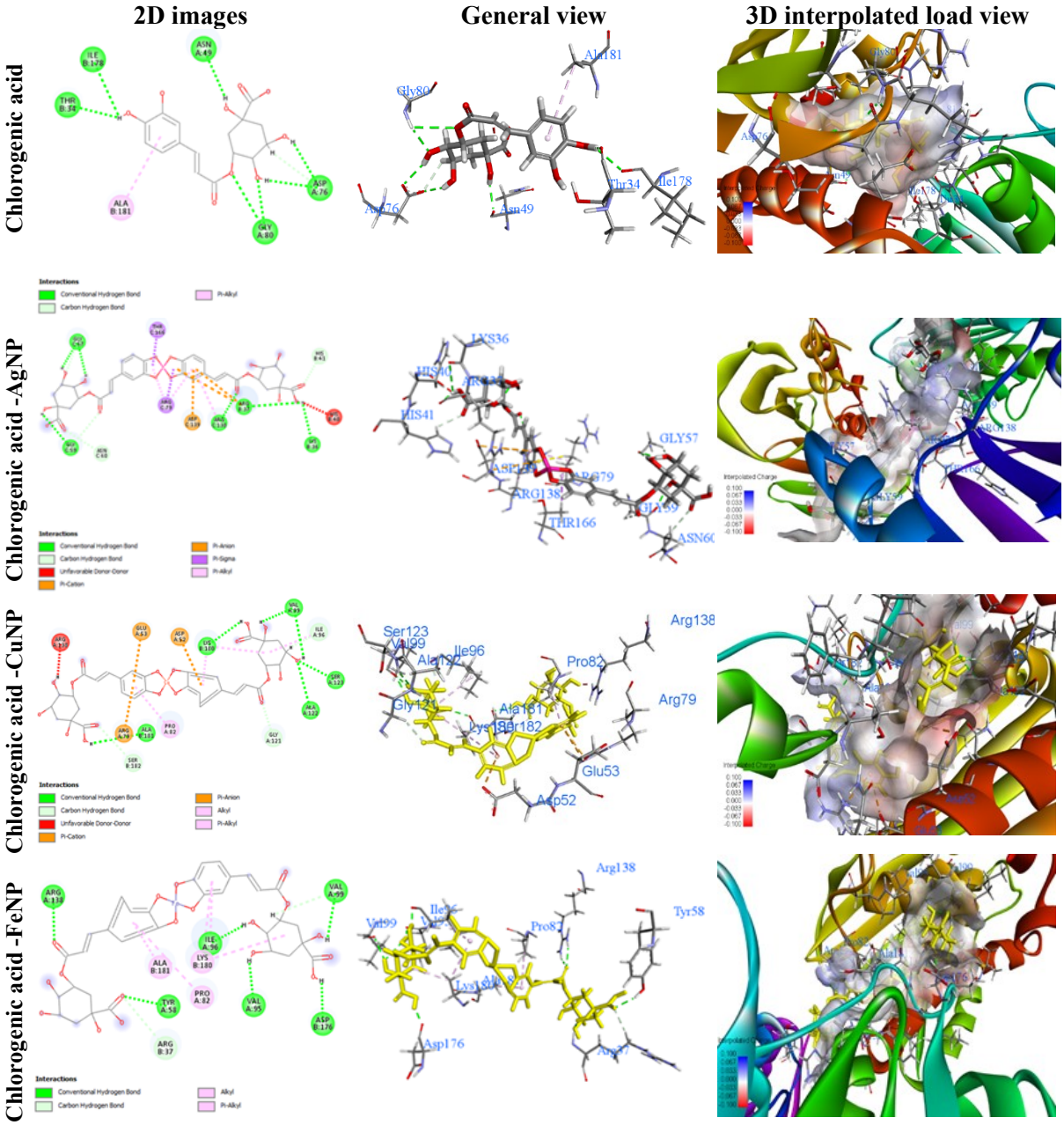

Figure 6. Interaction of chlorogenic acid and chlorogenic acid NPs with topoisomerase IV.

The MolDock score for the interactions of the chlorogenic acid-AgNP complex with the topoisomerase IV enzyme was calculated to be -136.424. Six conventional hydrogen bonds (ALA122, SER123, ALA181, LYS180, VAL99), three carbon-hydrogen bonds (GLY121, SER182, ILE96), one pi cation (ARG79), two pi anion interactions (ASP52, GLU53), two alkyls (LYS180, ILE96) and two pi-alkyls (PRO82, LYS180) interactions were detected between the chlorogenic acid-CuNPs complex and the active site of the enzyme topoisomerase IV. The MolDock score for the interactions of the chlorogenic acid-CuNPs complex with the topoisomerase IV enzyme was determined to be -159.261. Nine conventional hydrogen bonds (TYR58, ARG138, VAL99, VAL95, ILE96, ASP176), two carbon-hydrogen bonds (ARG37, VAL99), one alkyl (LYS180) and three pi-alkyl (ILE96, LYS180, ALA181) interactions were observed between the chlorogenic acid-FeNPs complex and the active site of the

topoisomerase IV enzyme (Figure 6). The MolDock score for the interactions of the chlorogenic acid-FeNPs complex with the topoisomerase IV enzyme was calculated to be 152.871 (Table 3).

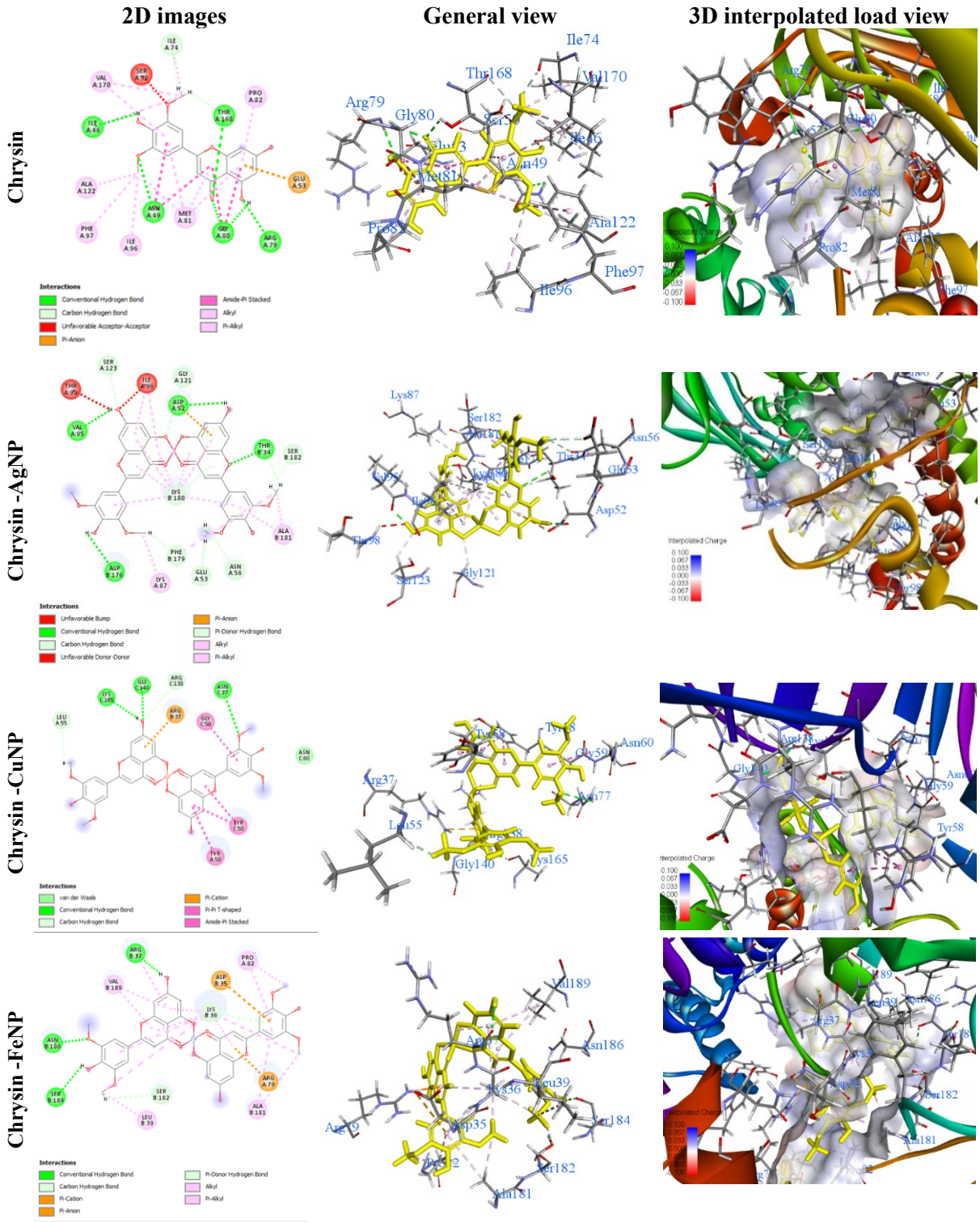

Figure 7. Interaction of chrysin and chrysin acid NPs with topoisomerase IV.

Six conventional hydrogen bonds (ASN49, ARG79, HLY80, THR168, GLY80, ILE46), two carbon-hydrogen bonds (ILE74, THR168), one pi-anion (GLU53), four amide-pi stacks (ASN49-SER50, GLY80-MET819), six alkyls (ALA122, ILE46, ILE74, VAL170, MET81, ILE96) and six pi-alkyl (PHE97, MET81, PRO82, VAL170) interactions were detected between chrysin and the active

site of the enzyme topoisomerase IV. The MolDock score for the interactions of chrysin with the enzyme topoisomerase IV was calculated to be -127.212.

Table 3. Category and MolDock score of molecules and molecule-NP complexes interactions with topoisomerase IV

Name	Category (type)	MolDock Score
Chlorogenic acid	GLY80, ASN49, ASP76,THR34, ILE78 (Conventional Hydrogen Bond) ASP76 (Carbon Hydrogen Bond) ALA181 (Pi-Alkyl)	-120.658
Chlorogenic acid-AgNP	ARG138, GLY57, LYS36, ARG37 (Conventional Hydrogen Bond) HIS41, GLY57, GLY59, ASN60 (Carbon Hydrogen Bond) ARG37 (Pi-Cation) ASP139 (Pi-Anion) ARG79, THR166 (Pi-Sigma) ARG79, ARG138 (Pi-Alkyl)	-136.424
Chlorogenic acid-CuNP	ALA122, SER123, ALA181, LYS180, VAL99 (Conventional Hydrogen Bond) GLY121, SER182, ILE96 (Carbon Hydrogen Bond) Pi-Cation (Pi-Cation) ASP52, GLU53 (Pi-Anion) LYS180, ILE96 (Alkyl) PRO82, LYS180 (Pi-Alkyl)	-159.261
Chlorogenic acid-FeNP	TYR58, ARG138, VAL99, VAL95, ILE96, ASP176 (Conventional Hydrogen Bond) ARG37, VAL99 (Carbon Hydrogen Bond) LYS180 (Alkyl) ILE96, LYS180, ALA181(Pi-Alkyl)	-152.871
Chrysin	ASN49, ARG79, HLY80, THR168, GLY80, ILE46 (Conventional Hydrogen Bond) ILE74, THR168 (Carbon Hydrogen Bond) GLU53 (Pi-Anion) ASN49-SER50, GLY80-MET81 (Amide-Pi Stacked) ALA122, ILE46, ILE74, VAL170, MET81, ILE96 (Alkyl) PHE97, MET81, PRO82, VAL170 (Pi-Alkyl)	-127.212
Chrysin-AgNP	THR34, ASP52, ASP176, VAL95 (Conventional Hydrogen Bond) GLY124, SER123, THR34, SER182, GLU53, ASN56, PHE179 (Carbon Hydrogen Bond) ASP52 (Pi-Anion) LYS180 (Pi-Donor Hydrogen Bond) ALA181 (Alkyl) ILE96, PHE179, LYS180, ALA181(Pi-Alkyl)	-155.737
Chrysin-CuNP	ASN77, GLY140, LYS165 (Conventional Hydrogen Bond) ARG138, LEU55 (Carbon Hydrogen Bond) ARG37 (Pi-Cation) TYR58 (Pi-Pi T-shaped) GLY59-ASN60 (Amide-Pi Stacked)	-128.930
Chrysin-FeNP	ASN186, ARG37, SER184 (Conventional Hydrogen Bond) SER182 (Carbon Hydrogen Bond) ARG79 (Pi-Cation) ASP35 (Pi-Anion) LYS36 (Pi-Donor Hydrogen Bond) LYS36, SLS181, LEU39, PRO82 (Alkyl) LYS36, VAL189, ARG37, PRO82, ALA181(Pi-Alkyl)	-142.414

Chrysin-AgNP interacting with the active site of topoisomerase IV enzyme showed four conventional hydrogen bonds (THR34, ASP52, ASP176, VAL95), nine carbon hydrogen bonds (GLY124, SER123, THR34, SER182, GLU53, ASN56, PHE179), one pi-anion (ASP52), one amino pi-donor hydrogen bond (LYS180), one alkyl (ALA181) and twelve pi-alkyl (ILE96, PHE179, LYS180, ALA181) interactions. The MolDock score of the interactions of Chrysin-AgNPs with topoisomerase IV enzyme was calculated as -155.737. Three conventional hydrogen bonds (ASN77, GLY140,

LYS165), two carbon-hydrogen bonds (ARG138, LEU55), one pi cation (ARG37), three pi-pi-shaped (TYR58) and one amide-pi stacked (GLY59-ASN60) interaction were determined between chrysin-CuNPs and the active site of the enzyme topoisomerase IV. The MolDock score for the interactions of chrysin-CuNPs with the enzyme topoisomerase IV was calculated to be -128.930. Chrysin-FeNPs interacting with the active site of the enzyme topoisomerase IV, three conventional hydrogen bonds (ASN186, ARG37, SER184), one carbon-hydrogen bond (SER182), one Pi cation (ARG79), one pi-anion (ASP35), one amino-pi-donor hydrogen bond (LYS36), five alkyls (LYS36, SLS181, LEU39, PRO82) and ten pi-alkyl (LYS36, VAL189, ARG37, PRO82, ALA181) interactions were observed (Figure 7). The MolDock score of the interactions of chrysin-FeNPs with the enzyme topoisomerase IV was calculated to be-142.414 (Table 3). The result of molecular docking showed that the molecule-particle complex has a higher ability to inhibit the enzyme. Therefore, it can be said that these complexes can be used in industrial fields.

4. Conclusion

In the case of cosmetic products and foodstuffs containing water, there is a risk that the product will spoil due to contamination during production, storage and transportation. The use of nanotechnology to effectively preserve food and cosmetics will increase the activity of antimicrobial agents and provide safer protection to the final product when integrated into packaging or film structures. In this study, the characteristic properties and biological activities of methanol extracts and NPs from green synthesis of *P. cognatum*, *M. pulegium* and *T. reticulatus* plants were investigated. In addition, the inhibitory properties of chlorogenic acid, chrysin and NPs complexes found as major components in the HPLC analysis of the plants against the enzyme topoisomerase IV were theoretically calculated by molecular docking. HPLC analysis revealed that the major component of *M. pulegium* and *T. reticulatus* was chrysin, while the major component of *P. cognatum* was chlorogenic acid. Antibacterial results showed that the extracts had no activity, while AgNPs and FeNPs had higher activity than CuNPs. Molecular docking results showed that chlorogenic acid-CuNPs (-159.261) and chrysin-AgNPs (-155.737) complexes had higher activity. It was also observed that the chlorogenic acid-CuNPs complex had a high score. It can be concluded that plant extracts with NPs have higher activity and therefore studies can be developed for their use in the food and cosmetics industry.

Acknowledgements

This research did not receive any funding. We would like to thank Prof. Dr. Ahmet Zafer TEL for her contributions to the identification of plant species.

References

Abdelsattar, A. S., Dawoud, A., & Helal, M. A. (2021). Interaction of nanoparticles with biological macromolecules: a review of molecular docking studies. *Nanotoxicology*, *15*(1), 66-95. https://doi.org/10.1080/17435390.2020.1842537

Acet, T., & Özcan, K. (2018). Investigation of some biological activities of horsetail (equisetum arvense) plant used for medicinal purposes in Gümüşhane province. *Turkish Journal of Agriculture-Food Science and Technology*, *5*(13), 1810-1814.

Amaliyah, S., Pangesti, D. P., Masruri, M., Sabarudin, A., & Sumitro, S. B. (2020). Green synthesis and characterization of copper nanoparticles using Piper retrofractum Vahl extract as bioreductor and capping agent. *Heliyon*, *6*(8). https://doi.org/10.1016/j.heliyon.2020.e04636

Ardakani, L. S., Alimardani, V., Tamaddon, A. M., Amani, A. M., & Taghizadeh, S. (2021). Green synthesis of iron-based nanoparticles using Chlorophytum comosum leaf extract: methyl orange dye degradation and antimicrobial properties. *Heliyon*, *7*(2). https://doi.org/10.1016/j.heliyon.2021.e06159

Arokiyaraj, S., Vincent, S., Saravanan, M., Lee, Y., Oh, Y. K., & Kim, K. H. (2017). Green synthesis of silver nanoparticles using Rheum palmatum root extract and their antibacterial activity against Staphylococcus aureus and Pseudomonas aeruginosa. *Artif Cells Nanomed Biotechnol*, *45*(2), 372-379. https://doi.org/10.3109/21691401.2016.1160403

Başar, Y., Gül, F., Nas, M. S., Alma, M. H., & Çalımlı, M. H. (2024b). Investigation of value-added compounds derived from oak wood using hydrothermal processing techniques and comprehensive analytical approaches (HPLC, GC-MS, FT-IR, and NMR). *International Journal of Chemistry and Technology*, *8*(1), 51-59. https://doi.org/10.32571/ijct.1365592

Başar, Y., Hosaflıoğlu, İ., & Erenler, R. (2024c). Phytochemical analysis of Robinia pseudoacacia flowers and leaf: quantitative analysis of natural compounds and molecular docking application. *Turkish Journal of Biodiversity*, *7*(1), 1-10. https://doi.org/10.38059/biodiversity.1446241

Başar, Y., Yiğit, A., Karacalı Tunç, A., & Sarıtaş, B. M. (2024a). Lavandula Stoechas extract; synthesis of silver nanoparticles (nature-friendly green synthesis method), characterization, antimicrobial activity and ın silico molecular docking study. *Current Perspectives on Medicinal and Aromatic Plants*, *7*(1), 24-33. https://doi.org/10.38093/cupmap.1461976

Chandraker, S. K., Lal, M., & Shukla, R. (2019). DNA-binding, antioxidant, H 2 O 2 sensing and photocatalytic properties of biogenic silver nanoparticles using Ageratum conyzoides L. leaf extract. *Rsc Advances*, *9*(40), 23408-23417.

Çoban, F., Tosun, M., Özer, H., Güneş, A., Öztürk, E., Atsan, E., & Polat, T. (2021). Antioxidant activity and mineral nutrient composition of Polygonum cognatum-a potential wild edible plant.

Çöteli, E., & Karataş, F. (2015). Yemlik (tragopogon reticulatus) bitkisinin yapraklarındaki glutatyon ve vitaminler ile toplam antioksidan kapasitenin araştırılması. *Gümüşhane Üniversitesi Fen Bilimleri Dergisi*, *5*(2), 78-86.

Dinesh, B., Monisha, N., Shalini, H., Prathap, G., Poyya, J., Shantaram, M., Hampapura, J. S., Karigar, C. S., & Joshi, C. G. (2022). Antibacterial activity of silver nanoparticles synthesized using endophytic fungus—Penicillium cinnamopurpureum. *Spectroscopy Letters*, *55*(1), 20-34. https://doi.org/10.1080/00387010.2021.2010764

Duncan, T. V. (2011). Applications of nanotechnology in food packaging and food safety: barrier materials, antimicrobials and sensors. *Journal of colloid and interface science*, *363*(1), 1-24. https://doi.org/10.1016/j.jcis.2011.07.017

Erenler, R., Yıldız, İ., Geçer, E. N., Kocaman, A. Y., Alma, M. H., Demirtas, İ., Başar, Y., Hosaflıoğlu, İ., & Behçet, L. (2024). Phytochemical analyses of Ebenus haussknechtii flowers: Quantification of phenolics, antioxidants effect, and molecular docking studies. *Bütünleyici ve Anadolu Tıbbı Dergisi*, *5*(2), 1-9. https://doi.org/10.53445/batd.1479874

Eruygur, N., Ucar, E., Ataş, M., Ergul, M., Ergul, M., & Sozmen, F. (2020). Determination of biological activity of Tragopogon porrifolius and Polygonum cognatum consumed intensively by people in Sivas. *Toxicology reports*, *7*, 59-66. https://doi.org/10.1016/j.toxrep.2019.12.002

Espinoza-Gómez, H., Flores-López, L. Z., Espinoza, K. A., & Alonso-Nuñez, G. (2020). Microstrain analyses of Fe3O4NPs greenly synthesized using Gardenia jasminoides flower extract, during the photocatalytic removal of a commercial dye. *Applied Nanoscience*, *10*(1), 127-140. https://doi.org/10.1007/s13204-019-01070-w

Eze, F. N., Jayeoye, T. J., & Eze, R. C. (2023). Construction, characterization and application of locust bean gum/Phyllanthus reticulatus anthocyanin - based plasmonic silver nanocomposite for sensitive detection of ferrous ions. *Environ Res*, *228*, 115864. https://doi.org/10.1016/j.envres.2023.115864

Gavande, N. S., VanderVere-Carozza, P. S., Hinshaw, H. D., Jalal, S. I., Sears, C. R., Pawelczak, K. S., & Turchi, J. J. (2016). DNA repair targeted therapy: The past or future of cancer treatment? *Pharmacology & therapeutics*, *160*, 65-83. https://doi.org/10.1016/j.pharmthera.2016.02.003

Hadi, M. Y., Hameed, I. H., & Ibraheam, I. A. (2017). Mentha pulegium: medicinal uses, anti-hepatic, antibacterial, antioxidant effect and analysis of bioactive natural compounds: a review. *Research Journal of Pharmacy and Technology*, *10*(10), 3580-3584.

Jara, Y. S., Mekiso, T. T., & Washe, A. P. (2024). Highly efficient catalytic degradation of organic dyes using iron nanoparticles synthesized with Vernonia Amygdalina leaf extract. *Scientific reports*, *14*(1), 6997. https://doi.org/10.1038/s41598-024-57554-5

Johnson, A., & Uwa, P. (2019). Eco-friendly synthesis of iron nanoparticles using Uvaria chamae: Characterization and biological activity. *Inorganic and Nano-Metal Chemistry*, *49*(12), 431-442. https://doi.org/10.1080/24701556.2019.1661448

Jyoti, K., Baunthiyal, M., & Singh, A. (2016). Characterization of silver nanoparticles synthesized using Urtica dioica Linn. leaves and their synergistic effects with antibiotics. *Journal of Radiation Research and Applied Sciences*, *9*(3), 217-227. https://doi.org/10.1016/j.jrras.2015.10.002

Katata-Seru, L., Moremedi, T., Aremu, O. S., & Bahadur, I. (2018). Green synthesis of iron nanoparticles using Moringa oleifera extracts and their applications: Removal of nitrate from water and antibacterial activity against Escherichia coli. *Journal of Molecular Liquids*, *256*, 296-304. https://doi.org/10.1016/j.molliq.2017.11.093

Kato, M. (2008). Chondrotoxicity of quinolone antimicrobial agents. *Journal of Toxicologic Pathology*, *21*(3), 123-131.

Kebede, O. G., Pasaoglulari Aydinlik, N., Oba, O. A., & Ertekin, E. (2024). Green synthesis and characterization of limonium sinuatum silver nanoparticles (AgNPs) for antioxidant and antimicrobial applications. *Analytical Letters*, *57*(16), 2773-2785. https://doi.org/10.1080/00032719.2024.2302074

Kuang, Y., Wang, Q., Chen, Z., Megharaj, M., & Naidu, R. (2013). Heterogeneous Fenton-like oxidation of monochlorobenzene using green synthesis of iron nanoparticles. *Journal of Colloid and Interface Science*, *410*, 67-73. https://doi.org/10.1016/j.jcis.2013.08.020

Kumar, B., Smita, K., Cumbal, L., & Debut, A. (2014). Sacha inchi (Plukenetia volubilis L.) oil for one pot synthesis of silver nanocatalyst: an ecofriendly approach. *Industrial Crops and Products*, *58*, 238-243. https://doi.org/10.1016/j.indcrop.2014.04.021

Kumar, P. V., Shameem, U., Kollu, P., Kalyani, R., & Pammi, S. (2015). Green synthesis of copper oxide nanoparticles using Aloe vera leaf extract and its antibacterial activity against fish bacterial pathogens. *BioNanoScience*, *5*, 135-139. https://doi.org/ 10.1007/s12668-015-0171-z

Mahiuddin, M., Saha, P., & Ochiai, B. (2020). Green synthesis and catalytic activity of silver nanoparticles based on Piper chaba stem extracts. *Nanomaterials*, *10*(9), 1777. https://doi.org/10.3390/nano10091777

Manikandan, A., & Sathiyabama, M. (2015). Green synthesis of copper-chitosan nanoparticles and study of its antibacterial activity. *Journal of Nanomedicine & Nanotechnology*, *6*, 1-5. http://dx.doi.org/10.4172/2157-7439.1000251

Miraj, S., & Kiani, S. (2016). Study of pharmacological effect of Mentha pulegium: A review. *Der Pharmacia Lettre*, *8*(9), 242-245.

Niraimathi, K., Sudha, V., Lavanya, R., & Brindha, P. (2013). Biosynthesis of silver nanoparticles using Alternanthera sessilis (Linn.) extract and their antimicrobial, antioxidant activities. *Colloids and Surfaces B: Biointerfaces*, *102*, 288-291. https://doi.org/10.1016/j.colsurfb.2012.08.041

Nkosinathi, D. G., Albertus, B. K., Jabulani, S. S., Siboniso Siphephelo, M., & Pullabhotla, R. V. (2020). Biosynthesis, characterization, and application of iron nanoparticles: In dye removal and as antimicrobial agent. *Water, Air, & Soil Pollution*, *231*, 1-10. https://doi.org/10.1007/s11270-020-04498-x

Okafor, F., Janen, A., Kukhtareva, T., Edwards, V., & Curley, M. (2013). Green synthesis of silver nanoparticles, their characterization, application and antibacterial activity. *International Journal of Environmental Research and Public Health*, *10*(10), 5221-5238. https://doi.org/10.3390/ijerph10105221

Öztürk, B. Y., Gürsu, B. Y., & Dağ, İ. (2020). Antibiofilm and antimicrobial activities of green synthesized silver nanoparticles using marine red algae Gelidium corneum. *Process Biochemistry*, *89*, 208–219. https://doi.org/10.1016/j.procbio.2019.10.027

Phan, H. T., & Haes, A. J. (2019). What does nanoparticle stability mean? *The Journal of Physical Chemistry C*, *123*(27), 16495-16507. http://dx.doi.org/10.1021/acs.jpcc.9b00913

Pinzi, L., & Rastelli, G. (2019). Molecular docking: shifting paradigms in drug discovery. *International Journal of Molecular Sciences*, *20*(18), 4331. https://doi.org/10.3390/ijms20184331

Prakash, P., Gnanaprakasam, P., Emmanuel, R., Arokiyaraj, S., & Saravanan, M. (2013). Green synthesis of silver nanoparticles from leaf extract of Mimusops elengi, Linn. for enhanced antibacterial activity against multi drug resistant clinical isolates. *Colloids and Surfaces B: Biointerfaces*, *108*, 255-259. https://doi.org/10.1016/j.colsurfb.2013.03.017

Prema, P. (2011). *Chemical mediated synthesis of silver nanoparticles and its potential antibacterial application.* InTech. doi: 10.5772/22114

Purniawan, A., Lusida, M. I., Pujiyanto, R. W., Nastri, A. M., Permanasari, A. A., Harsono, A. A. H., Oktavia, N. H., Wicaksono, S. T., Dewantari, J. R., & Prasetya, R. R. (2022). Synthesis and assessment of copper-based nanoparticles as a surface coating agent for antiviral properties against SARS-CoV-2. *Scientific reports*, *12*(1), 4835. https://doi.org/10.1038/s41598-022-08766-0

Rajesh, K., Ajitha, B., Reddy, Y. A. K., Suneetha, Y., Reddy, P. S., & Ahn, C. W. (2018). A facile bio-synthesis of copper nanoparticles using Cuminum cyminum seed extract: antimicrobial studies. *Advances in Natural Sciences: Nanoscience and Nanotechnology*, *9*(3), 035005.

Rathore, A., & Devra, V. (2022). Experimental investigation on green synthesis of FeNPs using Azadirachta indica leaves. *Journal of Scientific Research*, *14*(1), 375-386. https://doi.org/10.3329/jsr.v14i1.54344

Roy, A., Bulut, O., Some, S., Mandal, A. K., & Yilmaz, M. D. (2019). Green synthesis of silver nanoparticles: biomolecule-nanoparticle organizations targeting antimicrobial activity. *RSC Adv*, *9*(5), 2673-2702. https://doi.org/10.1039/c8ra08982e

Saravanan, M., & Nanda, A. (2010). Extracellular synthesis of silver bionanoparticles from Aspergillus clavatus and its antimicrobial activity against MRSA and MRSE. *Colloids and Surfaces B: Biointerfaces*, *77*(2), 214-218. https://doi.org/10.1016/j.colsurfb.2010.01.026

Serpi, M., Ozdemir, Z., & Salman, Y. (2012). Bazı bitki ekstrelerinin Propionibacterium acnes üzerine antibakteriyel etkilerinin araştırılması. *KSÜ Doğa Bilimleri Dergisi*, *15*(1), 7-12.

Skvarča, A. (2019). *Vrednotenje selektivnosti zaviralcev bakterijskih topoizomeraz* (Doctoral dissertation, Univerza v Ljubljani, Fakulteta za farmacijo).

Vakilzadeh, M. M., Heidari, A., Mehri, A., Shirazinia, M., Sheybani, F., Aryan, E., Naderi, H., Najaf Najafi, M., & Varzandeh, M. (2020). Antimicrobial resistance among community-acquired uropathogens in Mashhad, Iran. *Journal of Environmental and Public Health*, *2020*(1), 3439497. https://doi.org/10.1155/2020/3439497

Wang, W., Liu, L., & Han, Z. (2024). Effect of copper nanoparticles green-synthesized using Ocimum basilicum against Pseudomonas aeruginosa in mice lung infection model. *Open Chemistry*, *22*(1), 20240062.

Wolfgang, L. (2007). Bottom-up methods for making nanotechnology products. Access date: 15.08.2025. https://www.azonano.com/article.aspx?ArticleID=1079

Xia, X., Lan, S., Li, X., Xie, Y., Liang, Y., Yan, P., Chen, Z., & Xing, Y. (2018). Characterization and coagulation-flocculation performance of a composite flocculant in high-turbidity drinking water treatment. *Chemosphere*, *206*, 701-708. https://doi.org/10.1016/j.chemosphere.2018.04.159

Yenigun, S., Basar, Y., Ipek, Y., Gok, M., Behcet, L., Ozen, T., & Demirtas, I. (2024). A potential DNA protector, enzyme inhibitor and in silico studies of daucosterol isolated from six Nepeta species. *Process Biochemistry*, *143*, 234-247. https://doi.org/10.1016/j.procbio.2024.04.039

Yildiz, İ., Başar, Y., Erenler, R., Alma, M. H., & Calimli, M. H. (2024). A phytochemical content analysis, and antioxidant activity evaluation using a novel method on Melilotus officinalis flower. *South African Journal of Botany*, *174*, 686-693. https://doi.org/10.1016/j.sajb.2024.09.060